Copyright WILEY-VCH Verlag GmbH & Co. KGaA, 69469 Weinheim, Germany, 2015.

ADVANCED MATERIALS

Supporting Information

for *Adv. Mater.,* DOI: 10.1002/adma.201502546

Sequential Infiltration Synthesis of Doped Polymer Films with Tunable Electrical Properties for Efficient Triboelectric Nanogenerator Development

*Yanhao Yu, Zhaodong Li, Yunming Wang, Shaoqin Gong, and Xudong Wang**

Copyright WILEY-VCH Verlag GmbH & Co. KGaA, 69469 Weinheim, Germany, 2013.

Supporting Information

Sequential Infiltration Synthesis of Doped Polymer Films with Tunable Electrical Properties for Efficient Triboelectric Nanogenerator Development

*Yanhao Yu, Zhaodong Li, Yunming Wang, Shaoqin Gong, Xudong Wang**

Y. Yu, Z. Li, Prof. X.D. Wang,

Department of Material Sciences and Engineering,

University of Wisconsin-Madison, Madison, WI 53706, USA
E-mail: xudong@engr.wisc.edu

Dr. Y. Wang, Prof. S. Gong

Department of Biomedical Engineering and Wisconsin Institutes for Discovery,

University of Wisconsin-Madison, Madison, WI 53706, USA

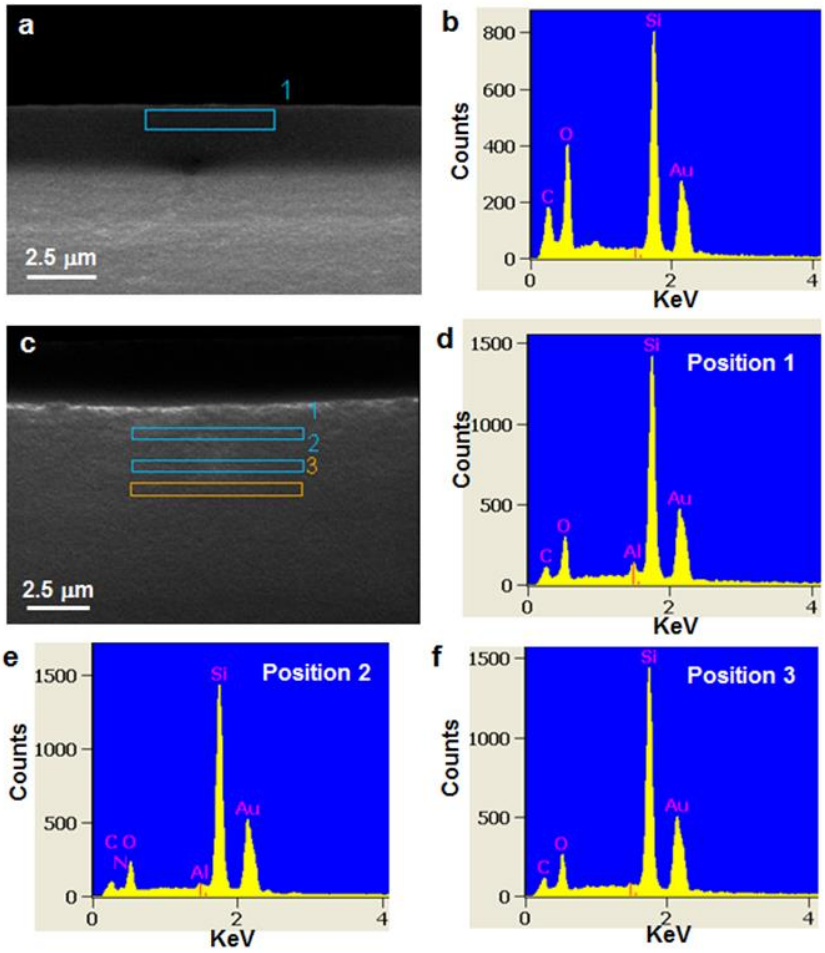

Figure S1. Elemental characterizations of AlO_x-doped PDMS film. (a) Cross-sectional SEM image of pristine PDMS. **(b)** Energy dispersive spectroscopy (EDS) spectrum of pristine PDMS (square box on figure S1a). No Al signal was detected. **(c)** Cross-sectional SEM image of AlO_x-doped PDMS. **(d-f)** EDS spectra obtained from positions 1 (d), 2 (e), 3 (f) on figure S1c. Al signal can be identified on position 1 and 2. No signal was detected on position 3, confirming the penetration depth of AlO_x was ~3 µm. C, O and Si signals were from PDMS and Au is from sputtering deposition for conductive purpose.

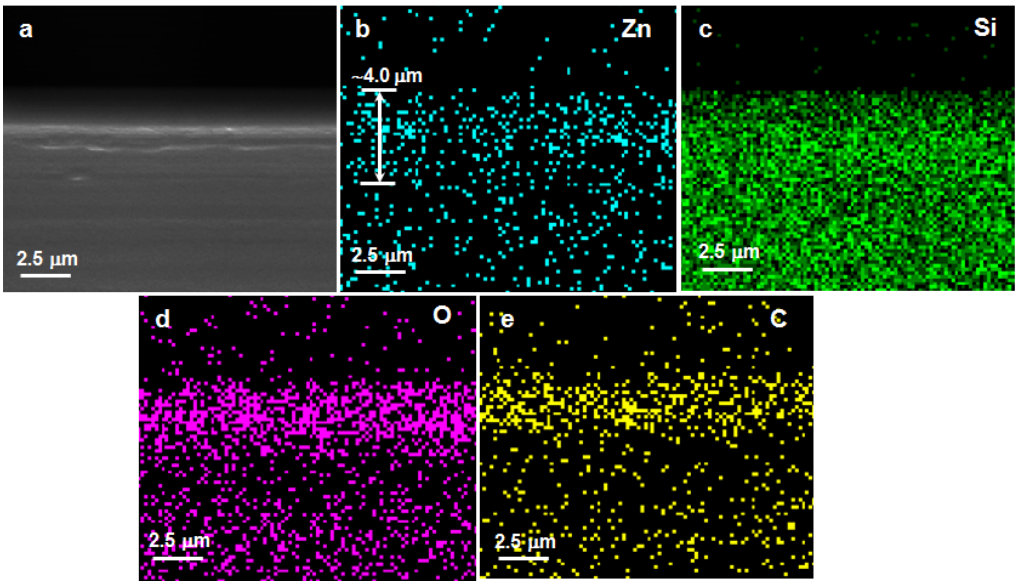

Figure S2. Elemental characterizations of ZnO_x-doped PDMS film. (a) Cross-sectional SEM image of ZnO_x-doped PDMS. **(b-e)** EDS mapping of ZnO_x-doped PDMS for (b) Zn, (c) Si, (d) O and (e) C elements.The traveling distance of Zn species was measured to be ~4.0 µm.

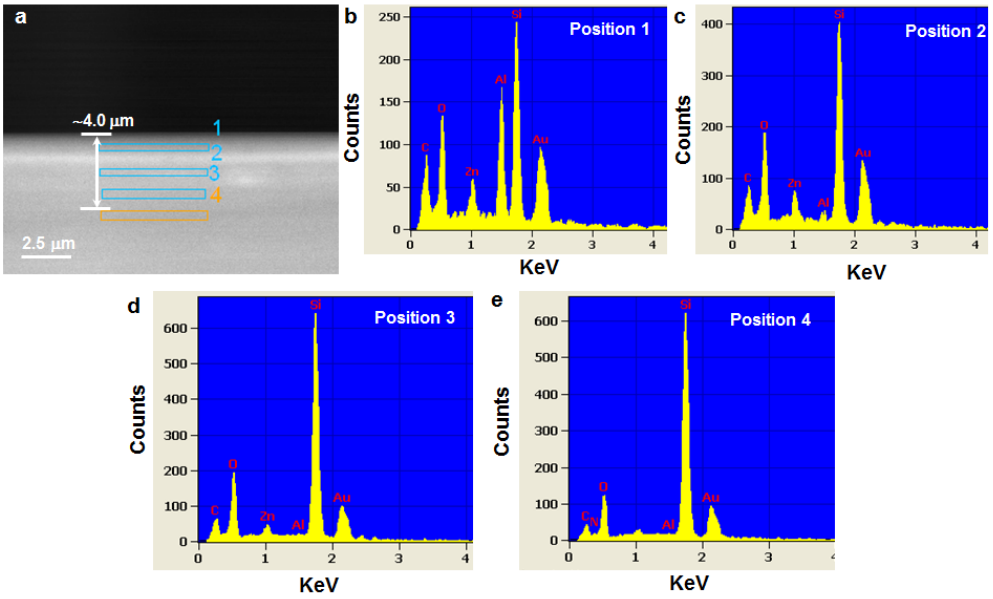

Figure S3. Elemental characterizations of ZnO_x-doped PDMS film. (a) Cross-sectional SEM image of ZnO_x-doped PDMS. **(b-e)** EDS spectra obtained from positions 1 (b), 2 (c), 3 (d), 4 (e) on figure S3a. Zn signal can be detected on position 1,2 and 3. No Zn signal appears on position 4, indicating the penetration depth of AlO_x was ~4 µm. C, O and Si signals were from PDMS and Au is from sputtering deposition for conductive purpose, and Al is from the sample stage.

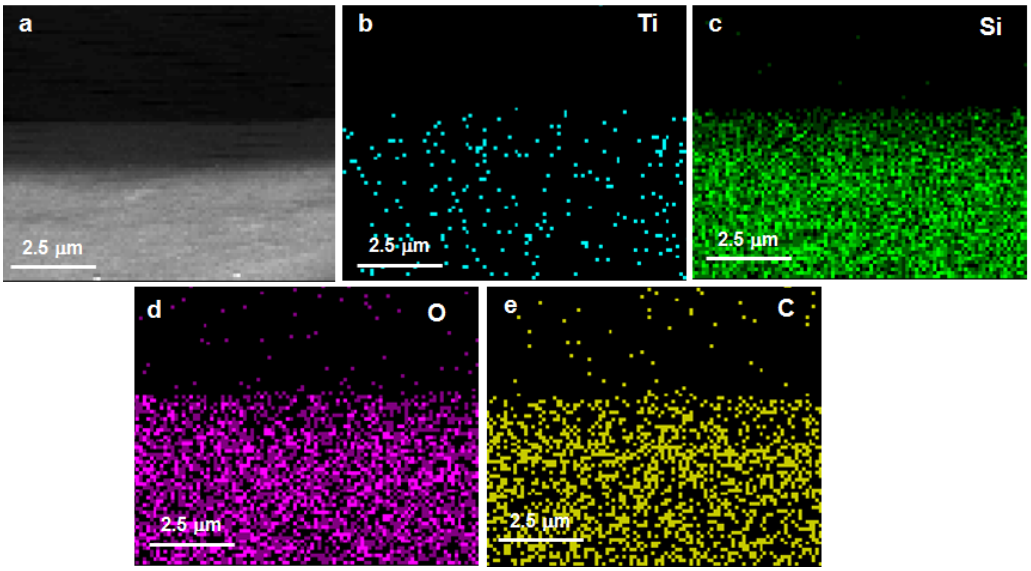

Figure S4. Elemental characterizations of $TiCl_4$ treated PDMS film. (a) Cross-sectional SEM image of $TiCl_4$ treated PDMS film. **(b-e)** EDS mapping of TiCl4 treated PDMS film for (b) Ti, (c) Si, (d) O and (e) C elements. No Ti signal was detected except noise.

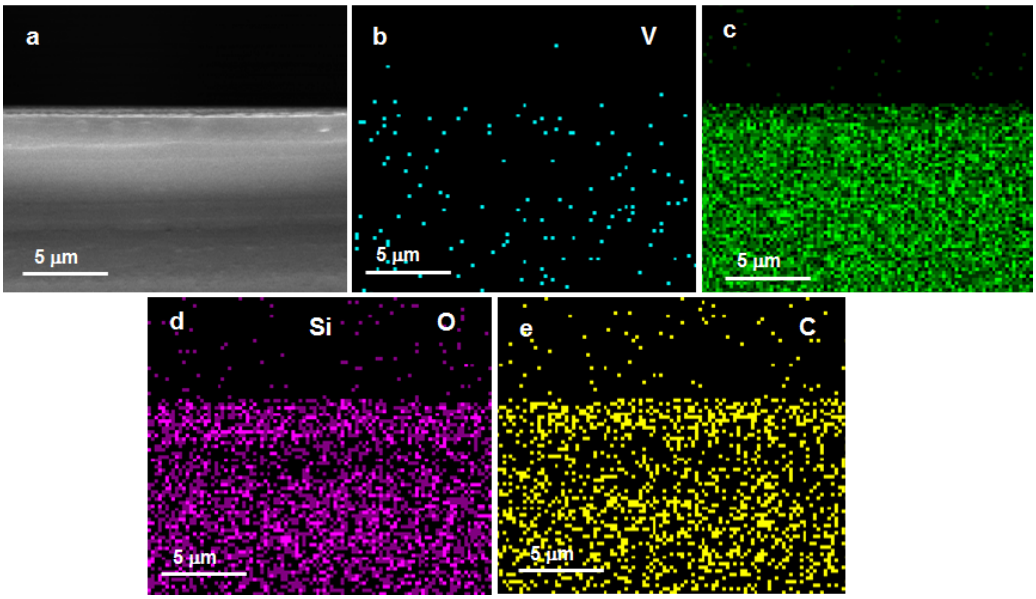

Figure S5. Elemental characterizations of $VOCl_3$ treated PDMS film. (a) Cross-sectional SEM image of $VOCl_3$ treated PDMS film. **(b-e)** EDS mapping of $VOCl_3$ treated PDMS film for (b) V, (c) Si, (d) O and (e) C elements. No V signal was detected except noise.

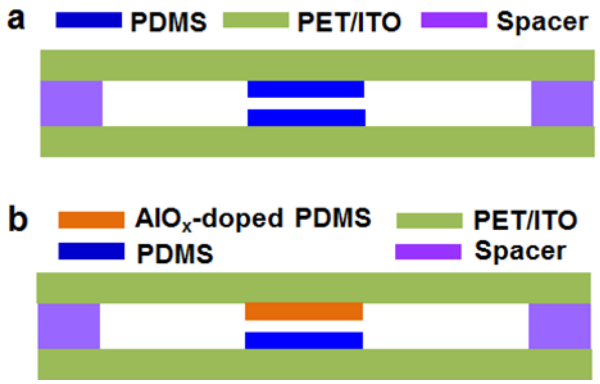

Figure S6. Schematic configuraitons of TENGs **(a)** PDMS-PDMS and **(b)** PDMS-AlO_x-doped PDMS. PDMS or AlO_x-doped PDMS were attached on the ITO surface on both top and bottom electrodes.

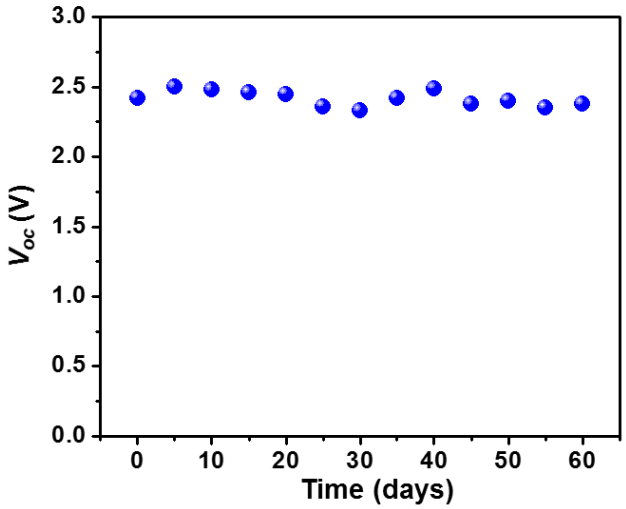

Figure S7. Stability test of TENGs assembled with AlO_x-doped PDMS. No deterioration of V_{oc} was found after repeat measurements in 60 days.

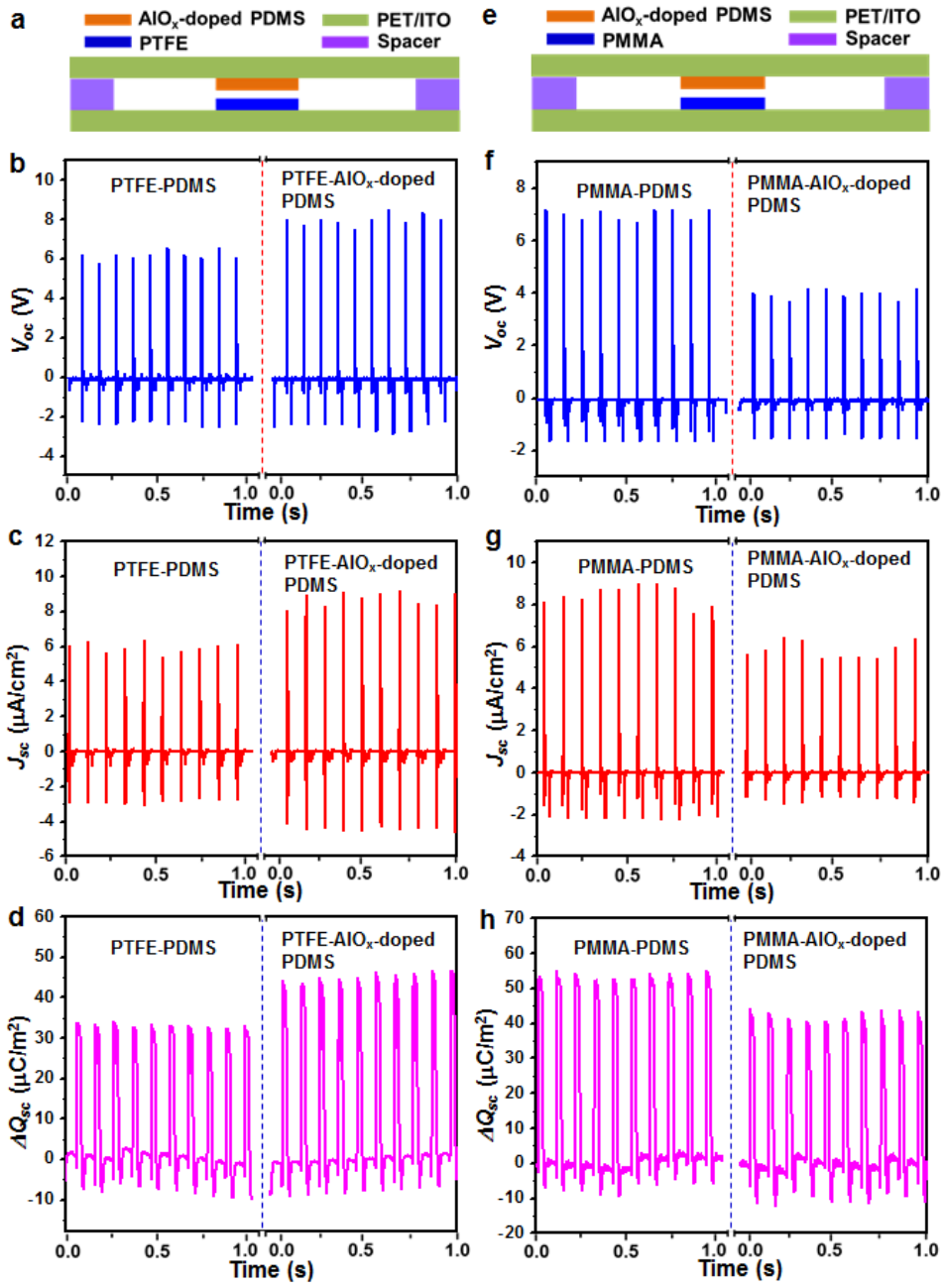

Figure S8. Design and performance of TENGs composed of PTFE-AlO_x-doped PDMS (a-d) and PMMA-AlO_x-doped PDMS triboelectric pairs (e-h). (a) Schematically illustration of TENGs with a configuration of PTFE/ITO/PET as the bottom electrode and AlO_x-doped PDMS/ITO/PET as the top electrode. **(b)** V_{oc}, **(c)** J_{sc} and **(d)** ΔQ_{sc} of TENGs made from PTFE-PDMS with and without AlO_x doping of PDMS. **(e)** Schematic of TENGs with a configuration of PMMA/ITO/PET as the bottom electrode and AlO_x-doped PDMS/ITO/PET as the top electrode. **(f)** V_{oc}, **(g)** J_{sc} and **(h)** ΔQ_{sc} characterizations of TENGs assembled from PMMA-PDMS with and without AlO_x doping of PDMS.

For the group of PDMS/PTFE, PDMS gave electron to PTFE during the periodical contact according to the triboelectric series.[1-3] As a consequence, PDMS and PTFE became positively charged and negatively charged, respectively. Compared with pristine PDMS, AlO_x-PDMS has stronger tendency to lose electron and therefore enabling a pronounced difference of surface charging condition between AlO_x-PDMS and PTFE, which resulting in larger V_{oc} (7.5 V), J_{sc} (8.2 μA cm^{-2}) and ΔQ_{sc} (44 μC m^{-2}) over that of pristine PDMS with V_{oc}

of 6.1 V, J_{sc} of 5.8 μA cm^{-2} and ΔQ_{sc} of 33 μC m^{-2}. On the other hand, for the group of PDMS/PMMA, PDMS need to attract electron from PMMA. The reduced electron acquiring capability of AlO_x-PDMS compared with that of pristine PDMS is expected to decrease the surface charge density of PDMS and thus diminishing the electric outputs. Under this circumstance, the AlO_x-PDMS yielded a V_{oc} of 3.9 V, a J_{sc} of 5.4 μA cm^{-2} and a ΔQ_{sc} of 38 μC m^{-2}, and pristine PDMS achieved a V_{oc} of 6.7 V, a J_{sc} of 8.3 μA cm^{-2} and a ΔQ_{sc} of 52 μC m^{-2}.

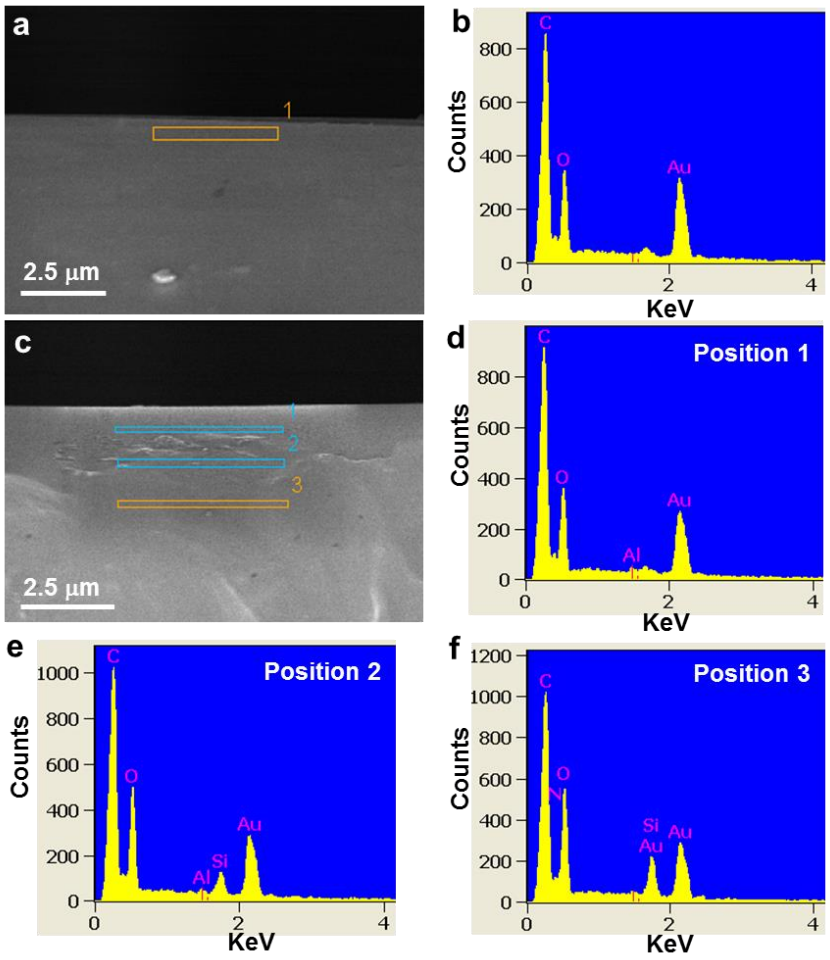

Figure S9. Elemental characterizations of AlO_x-doped Kapton film. (a) Cross-sectional SEM image of pristine Kapton. **(b)** EDS spectrum of pristine Kapton (square box on figure S9a). No Al signal was detected. **(c)** Cross-sectional SEM image of AlO_x-doped Kapton. **(d-f)** EDS spectra for positions 1 (d), 2 (e), 3 (f) on figure S9c. Al signal can be identified on position 1 and 2. It disappeared on position 3, suggesting the infiltration depth of AlO_x was ~3 μm. C, O and N signals are from Kapton. Si was from glass substrate and Au was from sputtering deposition for conductive purpose.

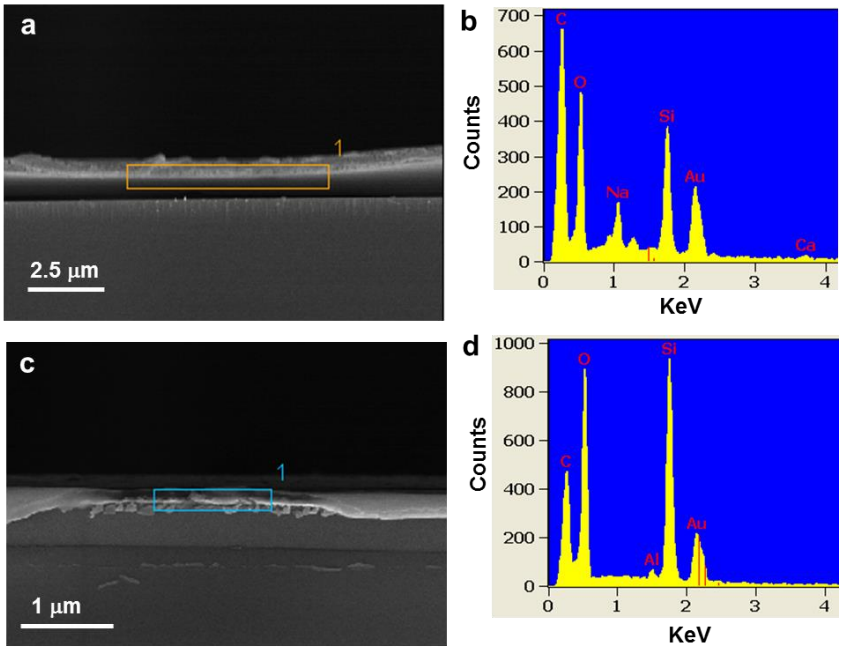

Figure S10. Elemental characterizations of AlO_x-doped PMMA film. (a) Cross-sectional SEM image of pristine PMMA. **(b)** EDS spectrum of pristine PMMA (square box on figure S10a). No Al signal was detected. **(c)** Cross-sectional SEM image of AlO_x-doped PMMA. **(d)** EDS spectrum of AlO_x-doped PMMA (square box on figure S10c). Clearly Al signal can be identified, indicating the successful introducing of Al element. C and O signals are from PMMA. Si and Na signals were from glass substrate. Au was from sputtering deposition for conductive purpose.

Reference:

[1] Z. L. Wang, *ACS Nano* **2013,** *7*, 9533.

[2] M. Kanik, M. G. Say, B. Daglar, A. F. Yavuz, M. H. Dolas, M. M. El-Ashry, M. Bayindir, *Adv. Mater.* **2015,** *27*, 2367.

[3] A. F. Diaz, R. M. Felix-Navarro, *J. Electrost.* **2004,** *62*, 277.